

A Major Project Report-II

on

**Modeling and Experimental Study of Temperature and  
Wear of Copper Alloy**

*Submitted for the partial fulfillment of the requirement for the degree of*

**Master of Technology**

in

**Computational Design**

*Submitted by*

**Abhishek Kumar Mahto (2K14/CDN/19)**

*under the supervision of*

**Sh. Krovvidi Srinivas  
(Assistant Professor)**



**Department of Mechanical Engineering**

**Delhi Technological University**

**July-2017**

## **DECLARATION**

I, **Abhishek Kumar Mahto**, hereby declare that the work presented in this thesis entitled “**Modeling and Experimental Study of Temperature and Wear of Copper Alloy**” is submitted for the partial fulfillment of the requirement to the degree of **Master of Technology (Computational Design)** in Department of Mechanical Engineering at **Delhi Technological University** is an authentic record of my own work carried out under the supervision of **Sh. Krovvidi Srinivas, Assistant Professor**. The matter presented in this thesis has not been submitted in any other University/Institute for the award of any degree or certificate. It is further declare that the matter has not been directly copied from any source without giving its proper reference.

**Signature of Student**

# **CERTIFICATE**



This is to certify that the dissertation entitled “**Modeling and Experimental study of Temperature and Wear of Copper Alloy**” submitted by **ABHISHEK KUMAR MAHTO (2K14/CDN/19)** in partial fulfilment of the requirements for the award of **Master of Technology in COMPUTATIONAL DESIGN** and submitted to the Department of Mechanical Engineering of Delhi Technological University (Formerly Delhi College of Engineering) is an authentic record of work carried out under the supervision of **Sh. K. Srinivas, Department of Mechanical Engineering.**

The information and data presented in this dissertation has not been submitted for the award of any other degree elsewhere.

**Sh. K. Srinivas (Project Mentor)**  
Assistant Professor  
Department of Mechanical Engineering  
Delhi Technological University  
Delhi-110042.

**Prof. R. S. Mishra**  
Head of Department  
Department of Mechanical Engineering  
Delhi Technological University  
Delhi-110042.



## **ACKNOWLEDGEMENTS**

Research is a higher concept. It brings to test our patience, vigor, and dedication. Every result arrived is a beginning for a higher achievement. My project is a small drop in an ocean. It needs the help of friends and guidance of experts in the field, to achieve something new.

I found my pen incompetent to express my thanks to my supervisor **Sh. Krovvidi Srinivas, Assistant Professor** under his kind and worthy guidance and supervision. I had the opportunity to carry out this work. It was only due to their advice, thoughtful comments, constructive criticism, and continuous vigil over the progress of my work with a personal interest that it has taken this shape. He has been a great source of encouragement.

To get an opportunity to carry out the project work in the well-equipped, ever developing laboratories in our institution, I would like to pay my deep sense of thankfulness to **Prof. R. S. Mishra, HOD, Department of Mechanical Engineering, DTU**.

I would like to express my sincere gratitude and indebtedness to **Prof. Vikas Rastogi, DTU** for prevailing me to do my laboratory work where I have completed my project work. I am very thankful to him that he allowed me to work in his lab and also for his guidance. I am also highly thankful to **Dr. R.C. Singh, Associate Professor, DTU**. He helped me and motivated me towards my work. His suggestion was very thoughtful and impressive from which I have inspired and able to complete my project.

I would especially thank to **Sh. Vipin Sharma, Assistant Professor, MAIT**. I have completed my project under their worthy guidance and supervision. Their advice and thoughtful comments inspired me and very helpful to complete my project.

I am very much thankful to my parents and family members for their moral support and encouragement, which was giving me the strength to chase my goal. Without their support and inspiration, I would not be able to complete my degree.

I would especially like to acknowledge my gratitude to all my dear friends for their consistent support, valuable suggestions from time to time to make this project worthy.

With a silent prayer to the Almighty, I take this opportunity to express my gratitude to all those who have supported me in completing my fourth-semester project work as a part of my degree program.

**ABHISHEK KUMAR MAHTO**  
**2K14/CDN/19**

# CONTENTS

Title.....	i
Declaration.....	ii
Certificate.....	iii
Acknowledgement.....	iv
Contents.....	v
List of figures.....	vii
List of tables.....	viii
Abstract.....	ix
<b>1. CHAPTER 1 - INTRODUCTION.....</b>	<b>1</b>
1.1 Tribology.....	1
1.2 Archard Wear law.....	4
1.3 Application of copper alloys.....	5
1.4 Simulia ABAQUS.....	5
<b>2. CHAPTER 2 - LITERATURE REVIEW.....</b>	<b>6</b>
<b>3. CHAPTER 3 - EXPERIMENTAL PROCEDURE.....</b>	<b>13</b>
3.1 Tribometer.....	13
3.2 Weighing Machine.....	13
3.3 Thermal Imaging Camera.....	14
3.4 Rockwell hardness test.....	14
3.5 Test Specimen.....	15
3.6 Pin of disc test experiment.....	16
3.7 Calculations.....	18
<b>4. CHAPTER 4 - ANALYSIS BY SIMULATION SOFTWARE.....</b>	<b>19</b>
4.1 Theory behind the POD Test Machine.....	19
4.2 Real Pin Wear.....	20
4.3 The ABAQUS-Model.....	21

4.3.1	The Part Module.....	21
4.3.2	Property Module.....	24
4.3.3	Assembly Module.....	24
4.3.4	Step Module.....	25
4.3.5	Interaction Module.....	25
4.3.6	Load Module.....	27
4.3.7	Mesh Module.....	30
4.3.8	Job Module.....	31
4.3.9	Visualization Module.....	32
4.3.10	Results.....	33
<b>5.</b>	<b>CHAPTER 5 - RESULTS &amp; DISCUSSION.....</b>	<b>36</b>
5.1	Wear rate.....	36
5.2	Temperature Variations.....	37
<b>6.</b>	<b>CHAPTER 6 - CONCLUSIONS AND FUTURE PROSPECTIVE.....</b>	<b>39</b>
<b>7.</b>	<b>REFERENCES</b>	

## LIST OF FIGURES

Figure 1.1	Simulation steps in ABAQUS	6
Figure 3.1	Digital weighing machine	13
Figure 3.2	Thermal imaging camera	14
Figure 3.3	The pin	15
Figure 3.4	The Disc	15
Figure 3.5	Experimental Setup	16
Figure 4.1	Static and dynamic friction forces	19
Figure 4.2	Forces acting on Pin and Disc Test	20
Figure 4.3	Behaviour of pin in wear process	21
Figure 4.4	The test disc in ABAQUS	23
Figure 4.5	Pin and Disc assembly	24
Figure 4.6	The boundary conditions for pin and disc	27
Figure 4.7	The pin on disc model showing maximum and minimum temperature	32
Figure 4.8	Frictional Dissipation Energy	34
Figure 4.9	Variation of Temperature	34
Figure 4.10	Average Contact Pressure	35
Figure 5.1	Wear rate variation with load	36
Figure 5.2	Wear rate variation with velocity	37
Figure 5.3	Temperature at velocity of 3.4m/s	37
Figure 5.4	Temperature at velocity of 4.6m/s	38
Figure 5.5	Temperature at velocity of 5.1m/s	38



## LIST OF TABLES

Table 3.1	Composition of alloy	15
Table 3.2	Values of Load, track distance, RPM and time for experiment	17
Table 3.3	Computation of wear rate and wear volume at different loads and speed	18
Table 4.1	Dimensions of the pin and disc used in the ABAQUS-model	22
Table 4.2	Part Properties	23
Table 4.3	Section name and its properties	24
Table 4.4	Step Properties	25
Table 4.5	Interaction Properties	26
Table 4.6	Constraint Properties	26
Table 4.7	Boundary Conditions	29
Table 4.8	Load	30
Table 4.9	Mesh properties	31
Table 4.10	Job Manager	31
Table 4.11	Output Request	32

## ABSTRACT

Study of wear in complex micro-mechanical components is often accomplished experimentally using a pin on- disc. The present thesis proposes an approach that involves a computationally efficient incremental implementation of Archard's wear model on the global scale for modeling sliding and slipping wear in such experiments.

This thesis comprises of detailed study with regard to the study of wear rate, friction force and coefficient of friction of copper alloy and mild steel with different parameters. It is a general observation that wear resistance is the key factor governing the applicability of the material as per various requirements. There have been a number of attempts to standardize the friction force and coefficient of friction by various committees. The tests were conducted on pin on disk apparatus with a cylindrical pin with flat circular disk placed perpendicular to the surface of the cylindrical pin in end as per ASTM G99.

The resulting wear depths obtained from experimental data is verified using finite element based numerical tools ABAQUS6.14 and implementing Archard's to calculate wear rate . The calculated wear rate from experiments and finite element tools are compared to check their validity. The wear rate was found to be maximum ( $0.4418\text{mm}^3/\text{s}$ ) for sliding velocity of  $5.1\text{m/s}$  at a load of  $10\text{kg}$  and minimum ( $5.95\text{e-}4\text{mm}^3/\text{s}$ ) for sliding velocity of  $3.4\text{m/s}$  at a load of  $8\text{kg}$ .

The wear rate was increasing with increase in the load and sliding velocity. The maximum temperature, at load of  $10\text{kg}$  with sliding velocity  $5.1\text{m/s}$ , was found to be equal to  $327\text{K}$  using ABAQUS which has little deviation from experimental value. This will be due to constant value of heat transfer coefficient taken in simulation.

# CHAPTER 1

## INTRODUCTION

### 1.1 Tribology

Tribology is the branch of science which deals with the study of interaction between contacting bodies and can be subdivided into three broad categories namely: friction, wear and lubrication. A brief outline of friction and wear is described below[1].

#### a. Friction

Friction is the resistance created at a contact interface to a relative tangential displacement of the two bodies. There are three main causes of friction:

- i) Adhesion
- ii) Ploughing
- iii) Asperity deformation.

The total friction can typically be approximated with sufficient accuracy by the sum of these components[2].

- i) **Adhesion** relates to the galling tendency of some materials. Junctions formed at asperity contacts due to normal load are deformed and later fractured by relative motion. As such adhesive friction is a function of both the interfacial shear strength and the surface energy of the contacting pair of materials.
- ii) **Ploughing** occurs either when one body is much harder than the other, or when hard wear particles are present, for example oxides. As the hard asperity/particle is traversed across the softer surface, the softer material is forced to deform plastically out of the path of the hard 'plough'. This friction component is principally a function of the hard asperity geometry; however, as wear progresses, the geometry is altered by the buildup of material on the plough. This partially explains why friction coefficient can change as wear progresses.
- iii) **Asperity deformation** generally forms the most significant portion of total friction in metallic contacts. This component arises from the deformations in asperities as they slide across each other such that compatibility is maintained.

Plasticity is a key feature in the friction components mentioned above, explaining its irreversible and dissipating nature. Plasticity itself is a complex subject[3]. A material's response will be altered by the material structure, both in terms of its crystal structure (e.g. dislocations, crystal size and orientation), temperature and loading history. It is therefore apparent that friction coefficient will not only be a function of original material condition (material combination, heat treatment, surface roughness etc) but will also be dependent on a number of environmental variables, and their histories such as sliding velocity, normal load, distance slid and temperature. From the above arguments it is clear that friction is complex phenomena. A model which can predict the behaviour of friction under a wide range of different conditions is not yet available. This is perhaps the justification for the enduring use of the Coulomb friction model, which is the most commonly used approximation of friction.

The Coulomb law assumes that the maximum shear load that can be sustained across the contact is proportional to the normal load. In reality there is a maximum load that can be transmitted, as the shear strength of the material is reached, hence a maximum shear stress  $\tau_{max}$  appears in some friction laws.

## **b. Wear**

Wear is a complex phenomenon which is not well understood. Humans have been aware of wear for many years[4]. It has been avoided by selecting harder materials for things that are more likely to wear. However, wear is not always something to be avoided, but many times it is desired; for example a pencil writes because the lead wears, and metal is polished by wearing the surface smooth. Despite of the fact that the occurrence of wear has been well documented throughout history, the scientific study of wear is relatively new. Because wear is such a new field of study, there is not always agreement on theories or meanings of terms, the classifications and definitions presented in this paper are by no means the only ones that have been proposed. The lack of understanding of wear is not only due to it not being studied; it is an inherently difficult phenomenon to study. Because wear occurs when objects are in contact, it is difficult to directly observe the process of wear as it happens. Therefore, experimenters generally rely on observations made after the test, and then infer what caused the wear. This is not the only difficulty; many of the causes and effects of wear only occur on a microscopic level. A third

reason that wear is not well understood is that it involves many different variables that make it difficult to generalize results. Following are the type of wear that can occur:-

- i) **Adhesive wear:** When two metals rub together with sufficient force to cause removal of material from low less hard material, adhesive wear occurs. This is dependent on physical and chemical factors such as material properties, velocity and applied load. Adhesive wear can cause problems such as cold welding, scoring pits, built up edges, etc. This type of wear can be prevented by selecting harder materials, selecting highly incompatible materials, selecting materials having low surface energy.
- ii) **Abrasive wear:** This type of wear occurs when hard surface slides across the softer surface.
- iii) **Surface fatigue :** Surface fatigue is a process by which the surface of a material is weakened by cyclic loading, which is one type of general material fatigue. Fatigue wear is produced when the wear particles are detached by cyclic crack growth of microcracks on the surface. These microcracks are either superficial cracks or subsurface cracks
- iv) **Fretting wear:** Fretting wear is the repeated cyclical rubbing between two surfaces. Over a period of time fretting which will remove material from one or both surfaces in contact. It occurs typically in bearings, although most bearings have their surfaces hardened to resist the problem. Another problem occurs when cracks in either surface are created, known as fretting fatigue. It is the more serious of the two phenomena because it can lead to catastrophic failure of the bearing.
- v) **Erosive wear:** Erosive wear can be defined as an extremely short sliding motion and is executed within a short time interval. Erosive wear is caused by the impact of particles of solid or liquid against the surface of an object. The impacting particles gradually remove material from the surface through repeated deformations and cutting actions
- vi) **Corrosive wear:** This kind of wear occurs in a variety of situations both in lubricated and unlubricated contacts. The fundamental cause of these forms of wear is chemical reaction between the worn material and the corroding

medium. This kind of wear is a mixture of corrosion, wear and the synergistic term of corrosion-wear which is also called tribocorrosion.

## 1.2 Archard wear law

The Archard wear law was originally proposed by Archard (1953), and validated against a wide variety of materials undergoing sliding wear by Archard & Hirst (1956), with Rabinowicz (1965) later extending the law to abrasive wear. The relation is the most common wear model, based on the principle that the rate of wear for a given material is proportional to the contact pressure and the slid distance, and inversely proportional to the hardness:

$$V = K \frac{PS}{H}$$

where,

$V$  = the worn volume,

$P$  = the normal load,

$S$  = total slid distance,

$H$  = material Hardness and,

$K$  = non dimensional constant of proportionality, termed the **wear coefficient**.

By assuming that the friction force is proportional to the normal load  $P$ , using Coulomb friction, the Archard wear law can be taken as indirectly relating the wear to the energy dissipated at the surface. Fouvry et al (1996) have developed a modified wear law which is based on this interpretation whereby the wear coefficient is based on the dissipated energy.

## 1.3 Application of Copper alloys.

Copper alloys has found increasing recognition for a wide variety of applications that requires resistance to mechanical wear, and though some very valuable research has been done in the

past, it is still not possible to conclude comprehensive published information on acceptable combinations of load, speed, temperature and lubrication for this range of alloys. It is to be hoped that further research will be done to establish these parameters for the benefit of designers. Nevertheless, some individuals and companies have found by experience that copper alloys provides a valuable alternative to more conventional materials for a number of specialized purposes and has become well established for high stress gears and bearings applications, notably in earth-moving equipment. But it is also used for a variety of less arduous applications such as: springs, wear strips, bushings, valve ship propellers, gears, bearing, sleeves and machine tools.

#### **1.4 Simulia Abaqus 6.14**

**Abaqus FEA** (formerly **ABAQUS**) is a software suite for finite element analysis and computational fluid dynamics. The Abaqus product suite consists of five core software products:

1. ***Abaqus/CAE***, or "Complete Abaqus Environment": It is a software application used for both the modeling and analysis of mechanical components and assemblies (pre-processing) and visualizing the finite element analysis result.
2. ***Abaqus/Standard***, a general-purpose Finite-Element analyzer that employs implicit integration scheme.
3. ***Abaqus/Explicit***, a special-purpose Finite-Element analyzer that employs explicit integration scheme to solve highly nonlinear systems with many complex contacts under transient loads.
4. ***Abaqus/CFD***, a Computational Fluid Dynamics software application which provides advanced computational fluid dynamics capabilities with extensive support for preprocessing and post processing provided in Abaqus/CAE.
5. ***Abaqus/Electromagnetic***, a Computational electromagnetics software application which solves advanced computational electromagnetic problems

Abaqus is used in the automotive, aerospace, and industrial products industries. The product is most popular with non-academic and research institutions in engineering because of the wide

material modeling capability, and its ability to be customized. Abaqus also provides a good collection of multiphysics capabilities, such as coupled acoustic-structural, piezoelectric, and structural-pore capabilities, making it attractive for production-level simulations where multiple fields need to be coupled.

### **Solution Sequence in abaqus**

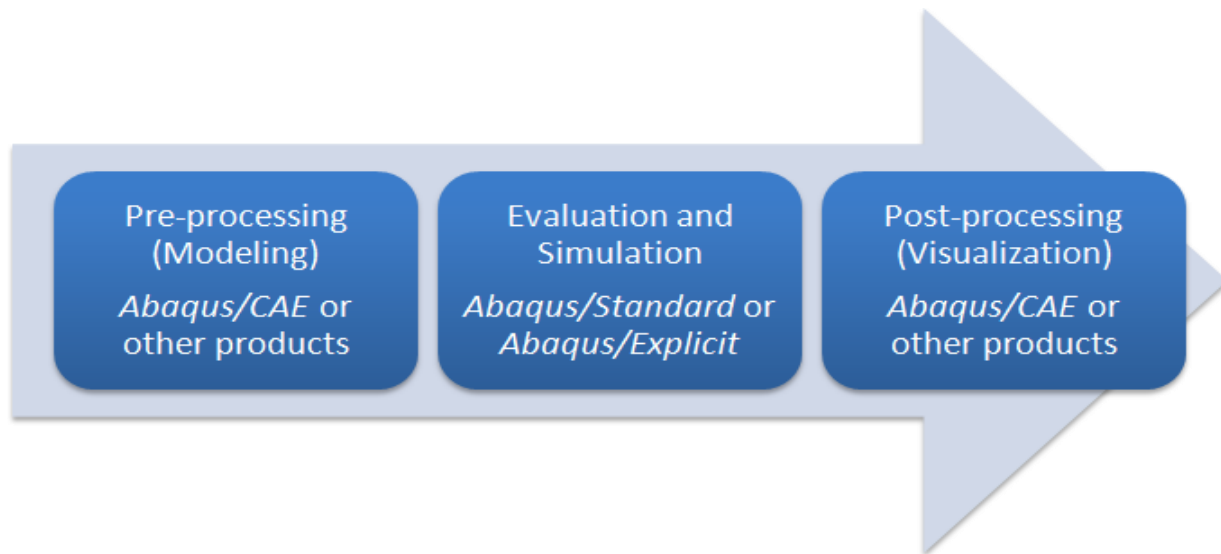


**Figure 1.1 Simulation steps in ABAQUS**

Simulation in Abaqus consists of three stages namely pre-processing, Evaluation and simulation and post-processing (visualization). In pre-processing model is build up in Graphic User Interface and loads & boundary conditions are applied. The next stage is creation of job and submit it for evaluation. The result can be seen from the post-processing module/visualization module. Different data like stresses, strains, temperatures, etc can accessed through History Output Request. These results are analyzed and conclusions are drawn.(Khot & Borah, 2015)



## CHAPTER 2

### LITERATURE REVIEW

#### 2.1 Literature of FEM

**Bortoleto et al. [6]** presented Experimental and numerical analysis of dry contact in the pin on disc test this work presents a computational study based on the linear Archard's wear law and finite element modelling (FEM), to analyse unlubricated sliding wear observed in typical pin on disc tests. Such modelling was developed using finite element software ABAQUSS with 3-Ddeformable geometries and elastic-plastic material behaviour for the contact surfaces. Archard's wear model was implemented into a FORTRAN user subroutine (UMESHMOTION) to describe sliding wear. Modelling of debris and oxide formation mechanisms was considered by the use of a global wear coefficient obtained from experimental measurements.

**Kennedy et al. [7]** carried out a research on Contact temperatures and their influence on wear during pin-on-disk tribotesting presents some of the most useful analytical and numerical methods that can be used to predict surface temperature rises in dry or boundary lubricated pin-on-disk tribotests. The development of relatively simple, accurate, and easy-to-use expressions that can be used to predict contact temperatures in pin-on-disk sliding contacts. Wear of a ceramic (zirconia), metal (stainless steel) and polymer (polyethylene) in pin- on-disc tests are carried out.

**Xinmin et al. [8]** uses of pin-on-disc, they studied the tribology characteristics of sintered versus standard steel gear materials and they simulate the sliding part of gear tooth contact in boundary and mixed lubricated regions, comparing the tribological characteristics of two sintered gear materials with those of a standard gear material. The comparison considered damage mechanisms, wear, and friction between these materials in different configurations (i.e., standard versus standard, sintered versus sintered, and sintered versus standard). The results indicate that, for pairings of the same gear materials, i.e., RS-RS (16MnCr5), AQ-AQ (Distaloy AQp0.2% C), and Mo-Mo (Astaloy 85Mop0.2% C), RS has a lower friction coefficient. For PM and RS combinations, both PM pins have lower friction coefficients with RS disc material than do RS

pins with PM disc materials. For the wear coefficient, at low and high speeds, RS pins always display better wear resistance than do AQ or Mo pins because of their high hardness and compacted microstructure. For RS–PM combinations, Mo pins display higher wear resistance than do AQ pins because their larger and more numerous pores enable good lubrication. Pins in the Mo–RS combination displayed the highest wear resistance, mainly because the pores in Mo discs hold lubricant, lubricating the contact surface and preventing adhesive wear. For the RS pin in the Mo–RS combination and the AQ pin in RS–AQ, the damage mechanism is slight adhesive wear and scuffing. For pins in the PM–PM, RS–PM, AQ–RS, and RS–RS combinations, the damage mechanism is a heavier scuffing-type adhesive wear.

**Verma et al. [9]**,Braking pad-disc system: wear mechanisms and formation of wear fragments. The tribological phenomena that occur in brake systems are interesting even in other respects than just the braking action. One important issue, that is gaining increasing importance over the last years, concerns the environmental impact of wear debris produced by the braking action. In this context, the present study is focused on the tribological behavior of a commercial friction pad material dry sliding against a cast iron disc. Pin-on-disc tests were conducted at room temperature under mild wear conditions, as concerns load and rotating speed. The effect of some components of pad material, of copper, on the dynamic of formation of tribological layer and wear debris is presented. The results obtained so, although referring to quite a simpler system than real brake systems, still may provide interesting indications, for instance in view of the development of novel brake pad materials and braking control systems.

**Zmitrowicz [10]**,A paper on ‘Wear patterns and laws of wear: a review’ presented that wear is a process of gradual removal of a material from surfaces of solids subject to contact and sliding. Damages of contact surfaces are results of wear. They can have various patterns (abrasion, fatigue, ploughing, corrugation, erosion and cavitation). The results of abrasive wear are identified as irreversible changes in body contours and as evolutions of gaps between contacting solids. The wear depth profile of a surface is a useful measure of the removed material. The definition of the gap between contacting bodies considers deformations of bodies and evolutions of wear profiles. The wear depth can be estimated with the aid of wear laws. Derived in this study, constitutive equations of anisotropic wear are extensions of the Archard’s law of wear.

The equations describe abrasion of materials with microstructures. The illustrative example demonstrates calculations of the abraded mass and temperatures in pinon-disc test rig.

**Guicciardi et al. [11]** performed ten pin-on-disk sliding wear tests for each experimental condition were carried out with a commercial tungsten carbide (WC) pin on silicon carbide (SiC) disks to determine the wear and friction data dispersion. The tests were repeated using two sliding speeds ( $v$ ), 0.1 and 1.0 m/s, and two applied loads ( $P$ ), 5 and 50 N. The wear data showed a dispersion in the range of 28–47 and 32–56%, for disk and pin, respectively. For the disk, the dispersion decreased when increasing both sliding speed and applied load; for the pin, no clear relationship was found. The friction values spread in the range of 5–15%, with a lower dispersion at high applied load, independent of the sliding speed. From a statistical point of view, it was found that, in all the experimental conditions adopted, about 20% of the wear and friction values can be considered outliers.

**PriitPodra et al. [12]** performed simulating sliding wear with finite element method, wear of components is often a critical factor influencing the product service life. Wear prediction is therefore an important part of engineering. The wear simulation approach with commercial finite element (FE) software ANSYS is presented in this paper. A modelling and simulation procedure is proposed and used with the linear wear law and the Euler integration scheme. Good care, however, must be taken to assure model validity and numerical solution convergence. A spherical pin-on-disc unlubricated steel contact was analysed both experimentally and with FEM, and the Lim and Ashby wear map was used to identify the wear mechanism.

It was shown that the FEA wear simulation results of a given geometry and loading can be treated based on wear coefficient<sup>2</sup>sliding distance change equivalence. The finite element software ANSYS is well suited for the solving of contact problems as well as the wear simulation. The actual scatter of the wear coefficient being within the limits of  $\pm 40$ –60% led to considerable deviation of wear simulation results. These results must therefore be evaluated on a relative scale to compare different design options.

**Prabhu [13]** Finite element analysis usually neglects the contributions of wear and the changes in the surface due to wear. However, wear may be important in any structure subjected to

repeated loadings and may be critical for certain tribological applications including the prediction of the sealing potential of surfaces. In this paper, a procedure is proposed whereby the effects of wear may be calculated and included in the overall analysis of the structure. The Archard's equation is used as the basis for calculating wear strain which is used to modify the elastic strain in an element in an explicit manner. Extensions of the theory are also proposed and an example using explicit creep for the wear adjustments is included.

**Imam Syafa et al. [14]** performed experiment two surfaces are brought in contact, deformation takes place at asperity level. The local pressure distribution and deformation of the contacting surfaces are importance with respect to wear. This paper describes a wear model to predict the wear of rough sliding contacts. The wear model is based on the general Archard's wear equation in combination with finite element analysis (FEA). In this paper, the roughness is represented by uniformly distributed spherical asperities. The proposed model, FE in combination with Archard's wear law, has proven to be a powerful tool in predicting wear of rough surfaces.

**Lim [15]** developed the wear map model, this paper presents a summary of the author's personal view of the development of wear-mechanism maps, culminating in the presentation of some recently proposed maps. These maps, present wear data in a graphical manner, can provide a more global picture of how materials in relative motions behave when different sliding conditions are encountered; they also provide the relationships between various dominant mechanisms of wear that are observed to occur under different sliding conditions as well as the anticipated rates of wear. Some thoughts on future directions for research are also presented.

**Pandey[17]** In this paper, tribo-potential of a combination of two solid lubricants (SLs) viz. a special graphite i.e. thermographite (TG) and hexa boron nitride (hBN) in a series of composites with fixed amount of short glass fibers (GF 30 wt. %) and Polyaryletherketone (PAEK- 50 wt.%) was investigated under severe operating condition (Load 900 N (Pressure-28 MPa), speed >1.6 m/s) against mild steel disc till the composites failed. It was observed that 20% of a single SL (either TG or hBN) did not show very good results, although TG inclusion proved better than hBN. When these two SLs (20%) were used in combination, synergistic effect was observed and best performance was exhibited by a composite containing 5% hBN and 15% TG with the

highest PV limits of 102.2 MPa m/s (900 N, 3.65 m/s) along with very low  $\mu$  (0.04) and specific wear rate ( $5.68 \times 10^{-16}$  m<sup>3</sup>/Nm), followed by composite with 10% TG and 10% hBN. Combination of 15% hBN and 5% TG stood next in performance. Synergism in tribo-performance due to combination of two SLs was reported for oils and friction materials but not for high performance anti-friction materials. Such composites have excellent potential as materials for dry bearings, gears etc. The Scanning electron microscopy (SEM) and Energy Dispersive X-ray analysis (EDAX) studies on worn surfaces proved beneficial to understand how the fiber-matrix bonding was affected due to different combinations of SLs and how it affected wear performance.

**Singh et al.[18]** Experiment was carried out on a pin-on-disc test rig. A textured mild steel disc containing dimples with a diameter of 420  $\mu\text{m}$  was considered with a mild steel cylindrical pin. Authors have observed that micro-dimple area density plays a major role in improving the coefficient of friction at the interface in boundary/mixed lubricating conditions. The dimple area density of 0.137 shows a lesser coefficient of friction in different zones of lubrication.

In starved lubrication the coefficient of friction increases with an increase of speed, which may be due to increase of shearing force or the contact of asperities. Wearing of the material was negligible up to a certain limit and afterwards rapid growth of specific wear rate took place, which may be due to breakage of the asperities in contact or lack of fluid film at the interface of the tribo-pair. During fully flooded conditions the coefficient of friction continuously decreases with speed and after a certain period it remains constant at a minimum value of nearly 0.03 while the specific wear rate decreases continuously to become constant after 11ms<sup>-1</sup>. This may be due to the formation of hydrodynamic lubrication at the interface of the pin and disc with the lubricant.

**Ying et al.[37]**, Heat flux of friction and the convective heat transfer coefficient were initially calculated accurately according to the theory of heat transmission. Then a pin-on-disk temperature field model was established via the finite element method, and the steady-state temperature distributions for the pin and the disk were analyzed. Due to the influence of the surrounding media on convective heat transfer, the center temperature in any section of a disk or pin specimen was highest and the temperature dropped gradually from inside out. The position

farther from the disk center was found with smaller temperature difference from the lubricating oil and smaller temperature dropping gradient. Under the impact of friction heat flow and convective heat transfer, the temperature of the pin-on-disk rose rapidly at the initial stage of friction, then increased at a slower rate, and finally reached a thermal equilibrium. Comparison between simulations and experiments for the average temperature rise at the disk bottom were in good agreement, which proved the correctness of the temperature model. This study provides references for temperature prediction in studying the pin-on-disk friction pair and verifies the feasibility of simulation method for studying the temperature field of friction pair

## **CHAPTER 3**

### **EXPERIMENTAL PROCEDURE**

#### **3.1 Tribometer**

A tribometer is a device/instrument that measures tribological quantities, such as coefficient of friction, frictional force, and wear volume, between the two contacting surfaces.

A pin on disc tribometer consists of a stationary "pin" and load is applied on its top surface due to which it makes contact with rotating disc. The cross section of the pin can be of any type but for simplification circular cross section is preferred over other sections. Coefficient of friction is determined by the ratio of the frictional force to the load applied on the pin[16].(Gmbh, n.d.)(Gmbh, n.d.)(Gmbh, n.d.)(Gmbh, n.d.)

#### **3.2 Weighing machine**

The weighing machine is used to measure the initial and final weights of the pin undergone wear phenomenon. This change in weight is used to calculate the wear rate and wear coefficient. In this machine a load cell will produce a small electric current when weight is placed. The electric is sent to the weight indicator and digital weight indicator will amplify the current and then translate it into digital weight. The least count of this machine is 0.0001g.



**Figure 3.1 Digital weighing machine**

### 3.3 Thermal Imaging camera

In order to get the temperature of the of the pin a thermal imaging camera is used. It is a non-contact type device that detects infrared energy (heat) given off by object. It has lenses just like other camera. But in this case lens focuses energy coming from the object. The sensors present convert the energy into electrical signals, which creates image. So the objects having higher temperature are shown in red color while that of the surrounding will appear varying shades of gray.



**Figure 3.2 Thermal imaging camera**

### 3.4 Rockwell Hardness test

Rockwell hardness test is used to determine the hardness of the test specimen. The Rockwell method measures the permanent depth of indentation produced by a force on an indenter. First, a preliminary test force is applied to a sample using a diamond indenter. This load represents the zero-reference position that breaks through the surface to reduce the effects of surface finish. After the preload, an additional load, called major load is applied to reach the total test load. This force is held for predetermined amount of time to allow for elastic recovery. This major load is then released and final position is measured against the position derived from the preload value and major load value. This distance is converted to a hardness number.

### 3.5 Test Specimen

Here sand casting method is employed to mold test specimen and then machining operations were performed in order to get the desired dimension of the product. Initially the test specimen



was casted in the form of cylindrical pin of copper alloy with proper allowances (Shrinkage and machining). Now it turned on lathe machine in order to reduce its diameter to 10mm and length of 32 mm. The rotating component is disc which is made of mild steel. The diameter of the disc was 165mm and depth 10mm.

**Composition of test specimen**

Elements	Carbon	Manganese	Silicon	Sulphur	Phosphorous	Copper
Percentage	0.937	0.316	0.230	0.007	0.017	98.493

**Table 3.1 Composition of alloy**



**Figure 3.3 PIN**

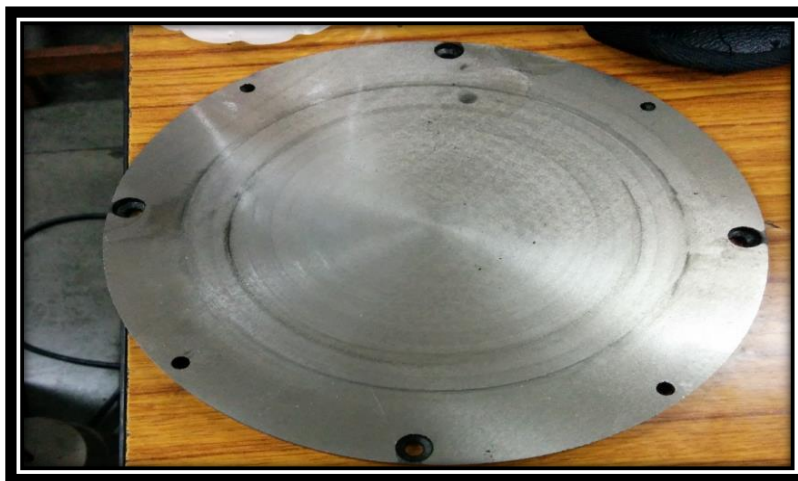


**Figure 3.4 DISC**

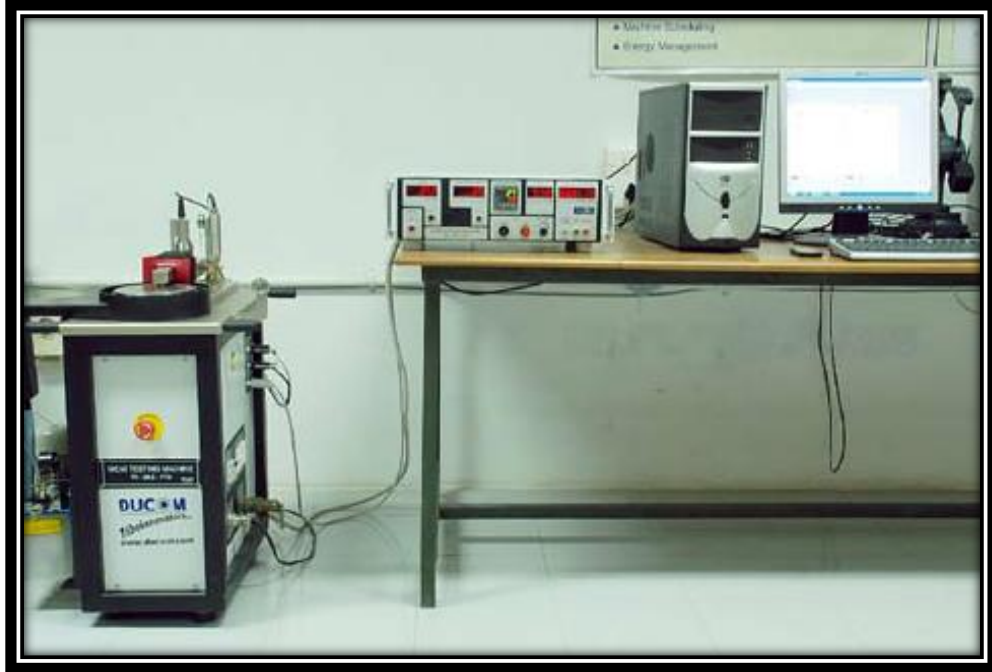


**Figure 3.5 EXPERIMENT SETUP**

### **3.6 Pin on Disc Test Experiment**

Pin on disc type wear monitor with data acquisition system was used to evaluate the wear behavior. Load was applied on pin using dead weight through pulley string arrangement. Dry sliding wear test was performed for a run of 2000m.



The machine is integrated with the computer using the software WINDCUM 2008. A window is open in the software and following fields can be varied[16]

- Load
- Time
- Pin diameter
- Track distance

The machine directly gives the friction force (in Newton) and wear depth (in micrometer) on the selected loading and sliding velocity. This machine basically consists of a rotating disc; and a pin is fixed over stainless steel pin holder. The rotating disc is fastened on the machine with the help

of screws. The load on the pin was applied using dead weight. The surface of the pin and disc was cleaned with acetone so that no asperities are present on it.

Following are the steps to perform the experiment:-

- Weigh the pin and note down its value.
- Now, the copper alloy pin was fixed on the pin holder using screw and load is applied. Start the **WINDCUM 2008** software and click on the refresh icon.
- Enter the **RPM, load, time (in seconds), pin diameter and track distance** and press **ACQUIRE**  icon.
- Click on  to bring origin to (0,0). As soon as the origin reaches zero click on **RUN**.
- The experiment has started and when time reaches half of the entered time click pictures of the setup from different angle to get the temperature of the contact point.
- As soon as the time ends, disc will stop. Remove the load and pin.
- Clean the pin with acetone and weigh it.
- The above procedure is repeated to get wear rate, coefficient of friction and reaction force at different loading conditions.
- Sliding distance was 2000m for the experiment.

S.No.	Track Distance(mm)	RPM	Load(kg)	Time(seconds)
1	130	500	10	588
2	130	500	9	588
3	130	500	8	588
4	110	800	10	435
5	110	800	9	435
6	110	800	8	435
7	90	1100	10	392
8	90	1100	9	392
9	90	1100	8	392

**Table 3.2 Values of Load, track distance, RPM and time for experiment**

### 3.7 Calculations

Density of the material is  $8850\text{kg/m}^3$

Therefore, Volume can be calculated by

$$\text{Volume} = \frac{\text{Mass}}{\text{Density}}$$

Wear rate can be calculated by

$$\text{Wear rate} = (\text{initial volume} - \text{final volume}) / \text{time}$$

Based on the data input to the tribometer following table can be obtained for temperature and wear rate.

S. No.	Initial Weight (grams)	Final Weight (grams)	Temperature(°C)		Change in mass (grams)	Change in volume (mm <sup>3</sup> )	Wear rate In (mm <sup>3</sup> /s)
			Maximum	Average			
1	21.2253	21.2180	45	41	7.3e-3	0.8241	1.42e-3
2	21.2180	21.2136	40	38	4.4e-3	0.4971	8.45e-4
3	21.1713	21.1682	43	37	3.1e-3	0.3503	5.95e-4
4	21.1682	20.3452	92	47	0.823	92.9943	0.2138
5	20.3452	19.7562	90	53	0.589	66.5536	0.1530
6	19.7562	19.4052	87	41	0.351	39.6610	0.0912
7	19.4052	17.8723	97	54	1.5329	173.2090	0.4418
8	17.8723	16.5465	92	53	1.3258	149.8087	0.3821
9	16.5465	15.3878	87	44	1.1587	130.9265	0.3339

**Table 3.3: Computation of wear rate and wear volume at different loads and speed**

## CHAPTER 4

### ANALYSIS BY SIMULATION SOFTWARE ABAQUS

#### 4.1 Theory Behind the PoD Test Machine

Before modeling FEA model in ABAQUS we need to understand the theory behind the Pin on Disc test setup. Therefore the Coulomb friction model theory will be explained. The real coefficient of Friction consists of two separate coefficient of Friction, first is static and other is dynamic coefficient of Friction. They have their own region in which they are applied. When the bodies are stationary (i.e. no relative movement occurs between the contacting bodies), the static coefficient of Friction is valid. When there is sliding contact between the bodies, the dynamic Coefficient of Friction is valid, see figure 4.1. In between there is transition region. The transition from static to dynamic friction results in a small startup error. Then there is no linear behavior. After that the dynamic coefficient of Friction becomes constant. In case of a fixed normal force, the reaction force of the static coefficient of Friction is not constant. It is dependent on the magnitude of the applied force and can be calculated with equation 4.1, it has a linear behavior[17]. The transition from the static to the dynamic friction has in the beginning a small startup error and then becomes constant and can be determined with the same equation, equation 4.1. The net force, which is available for the movement can be calculated with equation

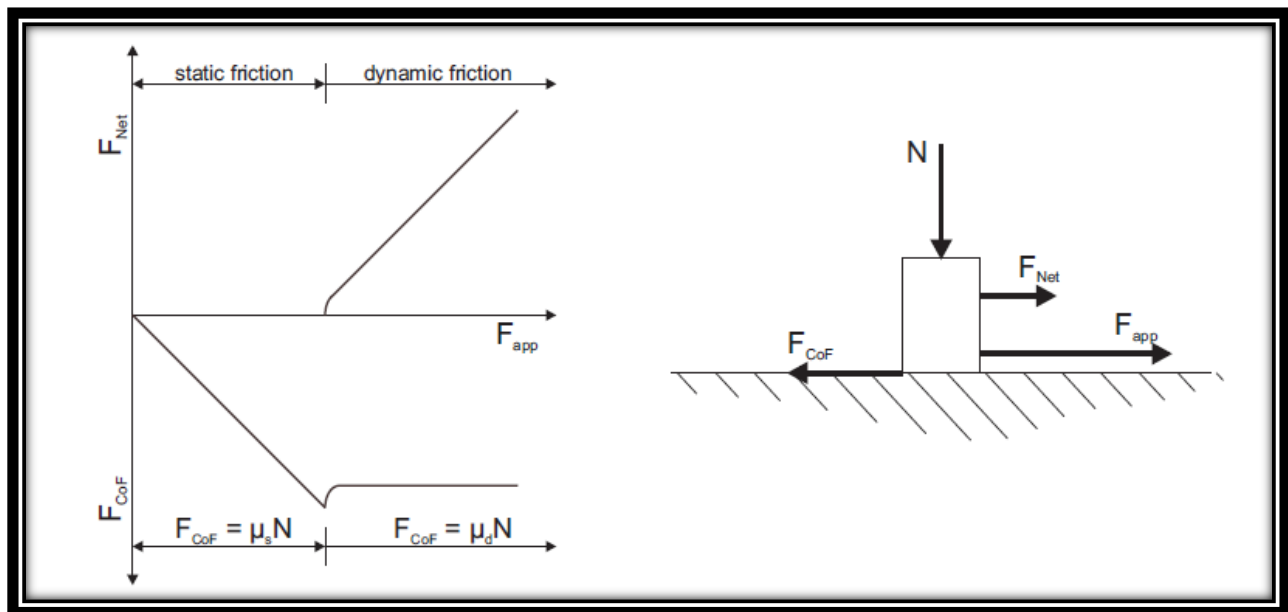


Figure 4.1: Static and dynamic friction forces

$$F_{CoF} = N * \mu \quad \dots\dots\dots 4.1$$

$$F_{Net} = F_{app} - F_{COF} \quad \dots\dots\dots 4.2$$

In figure 4.2 shows the forces that are acting in the Pin on Disc test. At the top of the pin, a force is applied, normal force  $N$ . The disc is rotating with a fixed RPM. Due to the normal force, the angular speed and the  $F_{CoF}$  a reaction force will occur. This reaction force is the friction force  $F_{CoF}$ .

The force that is applied at the disc surface,  $F_{app}$ , is the opposite direction of this force and is  $F_{CoF}$ . The torque force,  $F_T$ , is the same as the applied force,  $F_{app}$ , equation 4.2. This is force is larger than the friction force and can be compared with the applied force, equation 4.2. The force that is acting on the disc is reliant on the radius on which the pin is acting. The power required to drive the disc is the torque multiplied by the angular velocity.

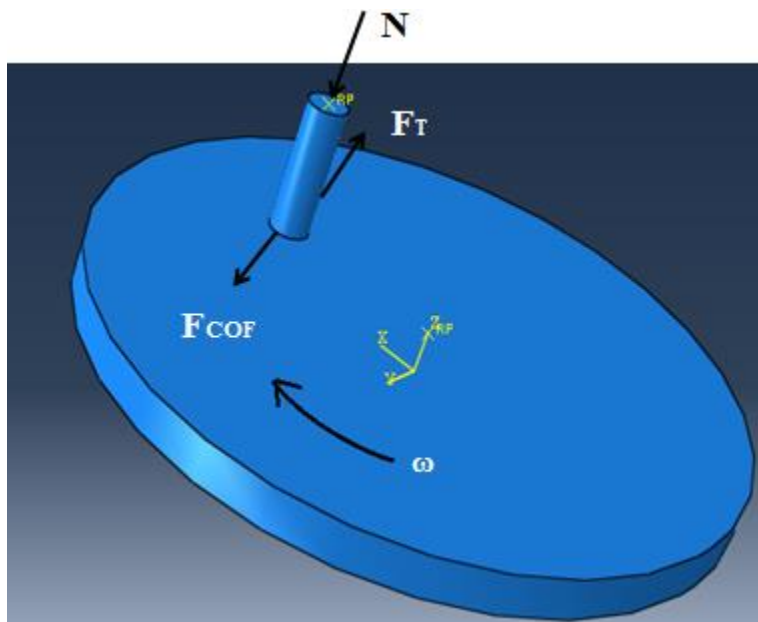


**Figure 4.2 Forces acting on Pin and Disc Test**

**4.2 Real Pin Wear**

Real pin wear can be divided into four phases. In first phase, the pin bends and only a small part of the pin will be in real contact with the disc. There will be no wear. In the 2<sup>nd</sup> phase the pin has been worn a little bit and more part of the pin surface is in contact with the disc. In the third phase, the surface will be wearing more. The complete surface of the pin will be in contact with

the disc, but there will not be yet steady state behavior. After a while the pin has been wearing more and the surfaces are polishing each other. This phase is called the steady wear phase, and the pressure is more or less constant in time. These four phases are represented in figure 4.3.

The arrow in the figure denotes the direction of movement of the disc and forces directions. During the tests a little bit of pin will be wear off the pin. The pressure distribution shown in this figure is the behavior that occurs when one material is used for the pin.

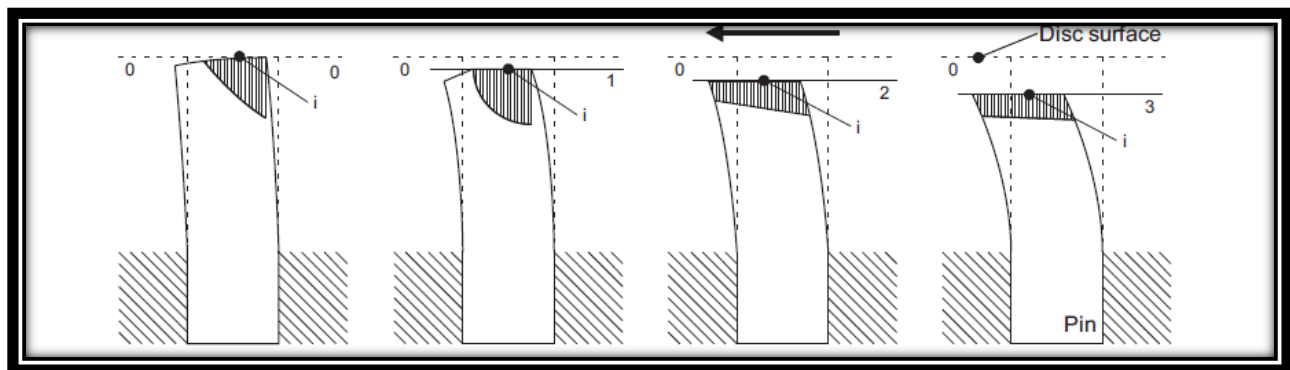


**Fig.4.3 Behavior of pin in wear process: (1) First contact; (2) Edge like contact, (3) Full contact Phase (4) steady wear phase**

### 4.3 The ABAQUS-Model

ABAQUS is a finite element program, which is used to perform the simulations of the Pin on Disc tests. There are three different stages in this program, to make, calculate and analyze the model. In the preprocessing phase, the physical model is developed. ABAQUS/CAE is used to do this. The real simulation is done in ABAQUS/standard[18,19]. This runs as a background process and does the real numerical calculations. Simulation of pin on Disc model is divided into two parts. First part consist of calculating the contact pressure and then using this contact pressure wear rate can be calculated. After the simulation is done the results can be monitored in the post-processing phase. ABAQUS/CAE is also used to view, plot and process the data.

#### 4.3.1 The Part Module

There are a number of ways to make or load parts into the part module. In ABAQUS there is a sketch feature, which makes it possible to draw the parts. Because the shapes of the parts are

very easy to draw, this feature is used. Modeling is done in millimeters or any other unit, accordingly the other quantities should be of the same order.

### **Modeling the pin**

Table 4.1 shows the real pin design dimension. The pin and clamp holder can be modeled in exactly that way in ABAQUS. This results in a very complex structure and strange structured elements. Time taken by CPU to solve this problem would be very large. Therefore, it is better to model the part of the pin that is outspreading the clamp and assign proper boundary conditions for the top surface. The pin is extends about 5mm. When a connection is made between the models, the contact surface area dimensions are the same, with similar contact behavior and probably pressure distribution. In this way it will be easier to compare the two models.

First a cross-section of the pin is drawn and then extruded to get the desired length. It is drawn at the position in the co-ordinate system, where it is situated in the assembly. Then only one translation will be needed to get the pin at desired position. The dimensions of the pin used in the FE-analysis are shown in table 4.1. In table 4.2, the properties of this part are shown. After extrusion of the cross-section, the part is intersected in four equal parts. By intersecting the pin, extra nodes appear that are needed to be able to apply the BC's at the top surface.

<b>The Disc</b>		<b>The Pin</b>	
<b>Radius</b>	165mm	<b>Diameter</b>	10mm
<b>Thickness</b>	10mm	<b>Height</b>	32mm

**Table 4.1: Dimensions of the pin and disc used in the ABAQUS-model**

### **Modeling the test disc**

Table 4.1 is also used in the modeling of the disc. The test disc is a circular disc with flat sides at a part of the outer radius. These flat sides are used for clamping the disc specimen onto the Pin on Disc test machine. When the disc is designed in its original way in ABAQUS, these flat sides' outcomes in homogenous elements, in case of the used square elements. All the elements will have the same shape by making the disc circular. The center of the pin acts at different track



diameter depending on load and RPM. The track on which the pin can run is 10millimeters wide. Out of the first results follows that this is more than enough to prevent stresses and deformations at the sides of the disc, since the Young's modulus of the disc is much larger than the Young's modulus of the pin. The thickness of the disc is also sufficient.

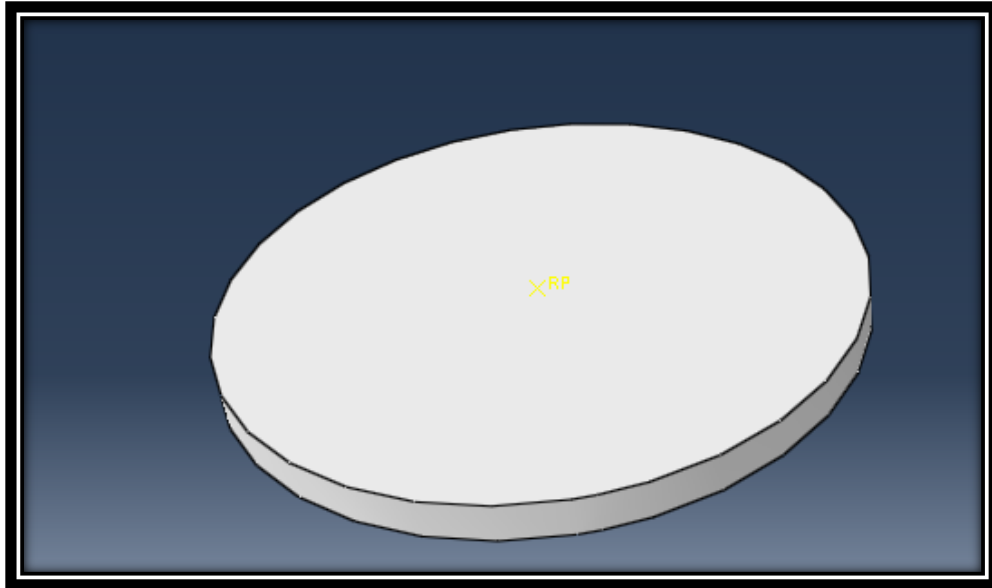


**Figure 4.4 The test disc in ABAQUS**

The dimensions of the pin and the disc used for modelling in ABAQUS-model are presented in Table 4.1. A sketch is made of the cross section of the body. This cross-section is extruded along the z-axis by providing the extrusion length. The settings for the disc are provided in Table 4.2. Next the disc is divided in four sections of 90degree. The model will not make a full circular movement; it will only rotate at most for 45degree. Within this region steady state behavior occurs and more data is not required. This is also done in order to get a short CPU-time. A fine mesh is generated for the portion of the disc which has physical contact with the pin surface. A RP (Reference Point) is constructed in the part module in order to control the movements of the disc. Several constraints are assigned to this RP in the interaction and load module.

Part Name	Modeling Space	Type	Base Feature	
			Shape	Type
Pin	3D	Deformable	Solid	Extrusion
Disc	3D	Deformable	Solid	Extrusion

**Table 4.2 Part Properties**

### 4.3.2 Property Module

In the property, module the different material properties are created and body sections are assigned to specified regions of the pin and the disc. The disc consists of one material and one section. The pin consists of other materials. The model the pin has as only one section and consists only of the copper alloy. In table 4.3 the different material properties are provided for pin and disc.

Section name	Material Behavior	Type	Young's Modulus	Poisson's ratio	Section
Pin	Material, Elastic	Isotropic	210GPa	0.3	Solid/Homogeneous
Disc	Material, Elastic	Isotropic	110GPa	0.34	Solid/Homogeneous

**Table 4.3 Section name and its properties**

### 4.3.3 Assembly Module

In this part a new co-ordinate system is created. The pin and disc will be loaded in this co-ordinate system and will be assigned to this co-ordinate system. First the disc part is loaded and positioned at the center of the co-ordinate system. Now the pin is brought into assembly. Using translation command pin position can be varied. It is then moved to proper track distance and contact is established between two mating parts.

In the assembly module it is also possible to create sets of lines, nodes and surfaces. These are useful to make it easier to select lines, nodes and surfaces when refining the mesh or assigning surfaces when the number of them arises and it becomes hard to select them separately each time. With fine meshes it is almost impossible to select every single object.

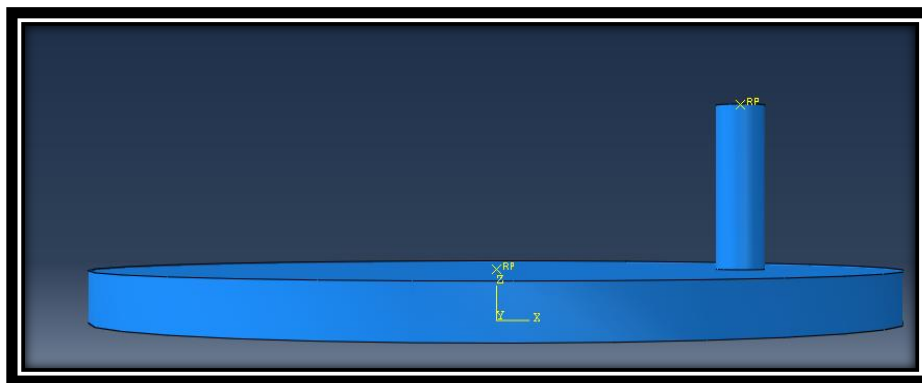


**Figure 4.5 Pin and disc assembly**

#### 4.3.4 Step Module

In this module different steps are created for analyzing. It is useful to make a single step for each change in the model. The output parameter can be prescribed in every step. Also the length of the step, the actual simulation time, can be set. As well as the start, minimum and maximum value of a single increment and the maximum number of increments can be assigned. In the initial step the model is checked or it is modeled in a correct way and if the output requests that are requested for each step are possible and no loads are applied during initial step. In the first step the force is applied at the top surface of the pin. Here a ramp function is used to apply the force. In the second step this force is still acting and the disc starts to rotate with a given RPM. The settings are provided in table 4.4.

Step	Step name	Procedure	Time	Maximum number of increments	Increment Size		
					Initial	Min.	Max.
0	Initial	Initial	N/A	N/A	N/A	N/A	N/A
1	Apply Pin Force	Themocoupled – temperature disp	1	10	0.1	0.1	1
2	Rotate Disc	Static, General	588	100	0.1	0.001	1

**Table 4.4 Step Properties**

#### 4.3.5 Interaction Module

**(a) Interaction of the surfaces:** There is a frictional contact between pin and the disc. The frictional property can be given in the interaction module. So a friction formulation is prescribed for the contact between the pin and the disc surfaces. There are a few models to prescribe the friction between the pin and disc. In the first model a penalty of 0.43 will prescribe, because this is the average coefficient of friction out of the results of the Pin on Disc test. In the beginning the friction in both directions (1st and 2nd-direction) is the same.

For the next model, a thorough research on the different friction models will be given. In table 4.5 the initial friction conditions are given.

<b>Interaction</b>	<b>Contact property</b>	<b>Friction formulation</b>	<b>CoF</b>
Pin Surface/Disc Surface	Tangential Behaviour	Penalty	0.43
Pin surface/disc surface	Normal Behaviour	Hard contact	N/A

**Table 4.5 Interaction Properties**

**(b) Disc rotation**

A coupling must be prescribed to control the movement of the disc. With the Reference Point assigned in the part module it is possible to control the disc by a single point, check table 4.6. The RP is set as the control point and the bottom surface of the disc is selected as the controlled region. The complete surface is selected because when only the outer region is selected the results will be influenced by the bending of the disc, which is neglected because it is not appearing. Now every single point on the surface has the same Boundary Condition's instead of only the outer region. A kinematic coupling is chosen instead of a distributing coupling. In case of a kinematic coupling all the DOF (Degrees Of Freedom) at the coupling nodes are eliminated and the coupling nodes will be constrained to move with the rigid body motion of the reference node. In case of a distributing coupling, the DOF are not eliminated, but are enforced in an average sense. This means that the resulting forces at the coupling nodes are equivalent to the forces and moments at the reference node and the force and moment equilibrium of the distributed loads about the reference point is maintained.(Baby & Jayadevan, 2013)

<b>Constraint</b>	<b>Constraint Type</b>
Disc/Reference Point	Coupling

**Table 4.6 Constraint properties**

### 4.3.6 Load Module

#### (a) Boundary conditions

To be able to simulate the clamping of the clamp holder it is important that the Boundary Conditions are chosen in a proper way. The Boundary Conditions should not generate extra stresses in the pin and it should be able to apply a load on the top surface of the pin. Coupling can't be used for the disc because then the material will not be able to move due to its Poisson ratio. Therefore the center node movements in the 1<sup>st</sup> and 2<sup>nd</sup> direction are suppressed and movement in the 3<sup>rd</sup> direction is free. The rotations about this vector are free as well. They are suppressed by the boundary conditions at the central partition lines. At the line in the direction of the rotation only the 1<sup>st</sup> direction is fixed and all the others are free. For the center line from the inner to the outer radius the 2<sup>nd</sup> direction is fixed. All these Boundary Condition's on the top surface together make sure that the surface is able to move towards the disc in the 3<sup>rd</sup> direction and that the surfaces of the pin and disc stay aligned. The Boundary Condition's make it also possible that the material can act to its poison ratio. So the material is able to deform. See figure 4.6 and table 4.7.(Baby & Jayadevan, 2013)(Baby & Jayadevan, 2013)(Baby & Jayadevan, 2013)(Baby & Jayadevan, 2013)

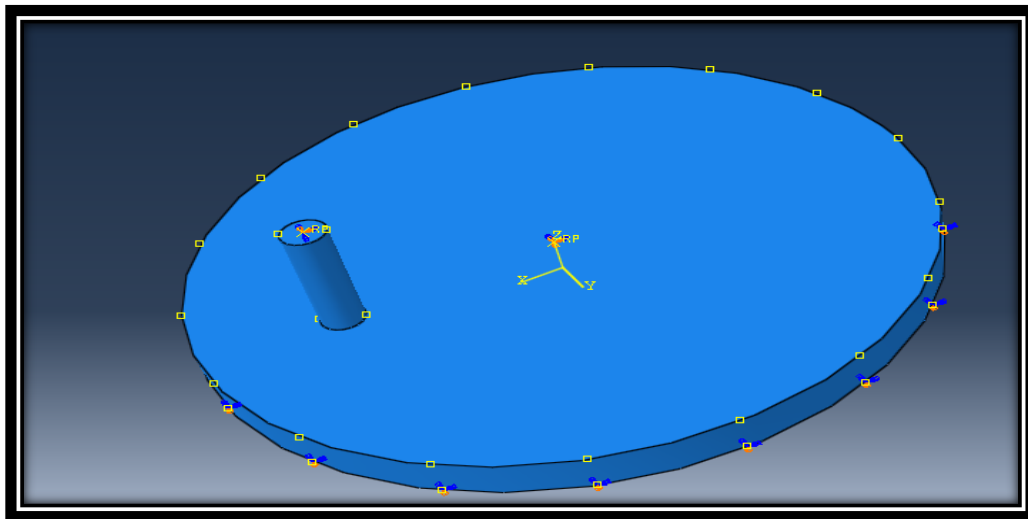


**Figure 4.6 The boundary conditions for pin and disc**

The previous described constraint on the disc is used in the load module. An angular velocity of 500,800,1100[rpm] are applied for the RP around the 3<sup>rd</sup>-direction axis. The other movements,

rotations and translation are restricted. This should be done because there is no counterattack at the disc shaft and in the clamp holder part as well. In figure 3.3 the boundary condition of the disc is shown. The purple surface is the controlled surface. The red dot below the disc is the Reference Point.

<b>Boundary condition</b>	<b>DOF</b>	<b>Initial Step</b>	<b>Step1</b>	<b>Step2</b>
<b>Pin Central Node</b>	U1	INACTIVE	X	Propagated
	U2		O	
	U3		X	
	UR1		O	
	UR2		O	
	UR3		O	
<b>Pin Front and Back node</b>	U1	INACTIVE	X	Propagated
	U2		O	
	U3		O	
	UR1		O	
	UR2		O	
	UR3		O	
<b>Pin left and right node</b>	U1	INACTIVE	O	Propagated
	U2		O	

	U3		X	
	UR1		O	
	UR2		O	
	UR3		O	
<b>Disc</b>	V1	INACTIVE	X	X
	V2		X	X
	V3		X	X
	VR1		X	X
	VR2		X	X
	VR3		X	RPM
<b>V= Velocity ( mm/s), U=Translation (mm), VR= Rotational speed (RPM)</b> <b>X= Fixed, O= Movement</b>				

**Table 4.7 Boundary Conditions**

**(b) Load**

There are two ways in which a force can be applied on the top surface of the pin. The 1st one is to make a force vector to act at a particular node. The 2nd option is by applying a pressure on the surface. The second one is the best. The 1st option results in a non-homogeneous force distribution in the upper part of the pin. When a pressure is applied at the top surface the size of the surface is of no importance because the quantity is prescribed in force per unit area and the pressure is distributed uniformly over the complete top surface. The value for the pressure is calculated using the formula given below. In figure 4.3 the applied pressure is only acting on the top surface in the figure to keep the figure clear. In the 1st step of applying the pressure it can be

seen that the pressure distribution is done in the right way, because the Von mises stresses at the top surface have all the same color. This means that the stresses have the same values.

$$Pr = \frac{N}{A} \dots\dots\dots 4.3$$

$$Pr = \frac{100}{7.85e-5} = 1.273e6MPa$$

Load condition	Direction	Step1	Step2
Pressure at top pin surface	Perpendicular to surface	1.273e6Pa	Propagated
Pressure at top pin surface	Perpendicular to surface	1.145e6Pa	Propagated
Pressure at top pin surface	Perpendicular to surface	1.018e6Pa	Propagated

**Table 4.8 Load**

**4.3.7 Mesh Module**

The element type used for meshing the assembly is **C3D6T** type. This is show in the table below. It is a continuum solid element. It has 6 nodes, at each corner 1. This is the best option, since the model is made in such a way that the elements are almost square in the contact region. This is required in order to get good results. The elements must be able to "feel" what is happening at the other side of the elements. This is not possible when the brick is very long and narrow, and the obtained results will be not very accurate. Another option is the **C3D6T**-element. This is a 6 node thermally coupled triangular prism element type. Baker has already researched this option and came to the inference that the C3D6T elements were the best option to perform the simulation. Because for further research the outcome of this research is going to be implemented in Baker' s model it is useful to use the same kind of elements. The comparison becomes easier when they are kept of the same element type.



Edges are seeded to get the desired number of elements on edges. This is performed by using seed edge command in mesh module. Another option is also available to seed the model. This is global seeding. Global seeding does not give much degree of freedom for meshing. Therefore for our purpose we are using local seed to create number of elements.

The edges are selected as sets edges with the same amount of desired elements on each edge. The pin consists of 286 elements in total. The elements are almost square. Since there is material removal going on when disc is rotating, so element deletion option is checked. With time mesh of the Pin Keep on change so dynamic meshing is used for this model. These elements have physical contact with the pin. The elements of this part are almost square, except of a small angle. The elements of this part of the disc have almost the same size as the pin elements. Then the calculations will run smoother and give more accurate results, because every node of the pin has contact with a corresponding node on the disc surface.

<b>Part name</b>	<b>Element Type</b>	<b>Element Type Description</b>
<b>Disc</b>	C3D6T	6 node thermally coupled triangular prism
<b>Pin</b>	C3D6T	6 node thermally coupled triangular prism

**Table 4.9 Mesh Properties**

#### **4.3.8 Job module**

After finishing the physical modeling, the job is created and data is checked. The job is now submitted for analysis. The program will check if all settings are correct. Also will be checked if the requested output variables are available for the model. The 1st jobs run on a computer with 4 parallel processors and the memory the program is allowed to use is set on 90% of the available RAM. Since it is a complex program, it will run slowly. During analysis, the analysis can be checked with the monitor function. The progression of the analysis is shown. The settings for this module are shown in table 4.10.

<b>Job Name</b>	<b>Model</b>	<b>Type</b>	<b>Run Mode</b>
<b>Wear</b>	Model-1	Full Analysis	Background

**Table 4.10 Job Manager**

### 4.3.9 Visualization module

The output parameters are selected in the step module. The parameters in table 4.11 are of importance in this analysis[22]. The values that are computed in ABAQUS6.14 are verified with analytical results.

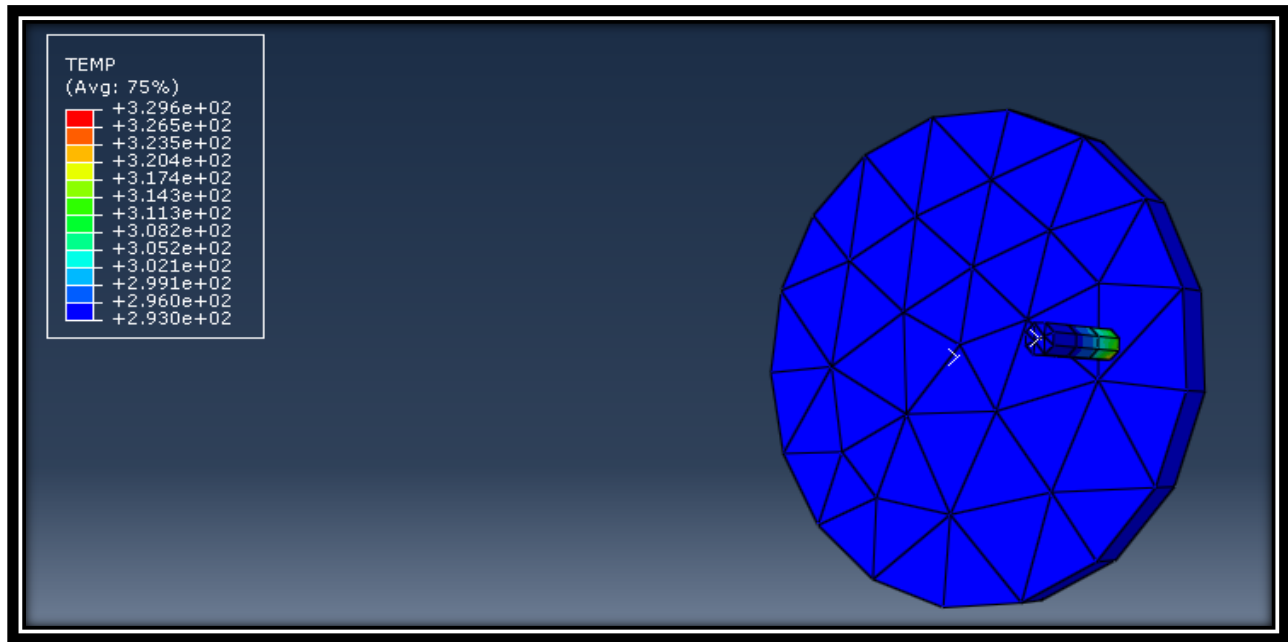


Figure 4.7 The pin on disc model showing maximum and minimum temperature

Output Request	Abbreviation	Description	Save Output data
<b>Frictional dissipation</b>	ALLFD for whole model	The energy that is dissipated into heat	Every Increment
<b>Translation</b>	U1	Translation in 1 <sup>st</sup> direction	
	U3	Translation in 3 <sup>rd</sup> direction	
	UR3	Rotation in 3 <sup>rd</sup> direction	
<b>Reaction Forces</b>	CSHEAR1	Reaction forces in 1 <sup>st</sup> direction	
	CSHEAR2	Reaction forces in 3 <sup>rd</sup> direction	
<b>Contact Pressure</b>	CPRESS	Contact Pressure between pin and disc	

Table 4.11 Output request

#### **4.3.10 Results**

Observing the animation of the simulation makes clear that the boundary conditions of the pin are applied properly. There are no any extra stresses generated around the boundary conditions at the top of the pin. When a plot is made of the nodes at the lower surface of the disc part of the 3rd-direction, no meaningful displacement occurs. This means that the BC of the disc is chosen in the right way as well.

In the first step the pressure is nicely equally distributed, because the model has one color at each increment, the von Mises stresses are of the same magnitude in every point in the pin. This is what is desired. There is symmetric spot of stresses in the disc around the pin when viewed from the top, That it is completely round is due to circular form of the pin. Large stresses occur only in the upper part of the disc.

In the second step the von Mises stresses for the pin are similar in what can be found in. High stresses occur at the front of the pin and low stresses at the back. It look as if the model is modeled in a right way, but to make sure it is a good model, the values should be compared to experimental values.

The stresses inside the pin are higher than the outside of the pin. When the disc rotates and the normal force is pushing at the top of pin, the pin tries to stick, together with the movement. It causes a little bending of the pin. Due to friction between the two surface wear occurs and heat is also generated.

To make sure that the model is correct the different values of the quantities have to be checked. The values that will be checked are summarized below. An approach of what the values should be, are calculated with the equations presented in chapter 1. The prescribed values should have a certain value at a certain point in the simulation.

- 1.** Frictional energy dissipation
- 2.** Temperature
- 3.** Contact pressure

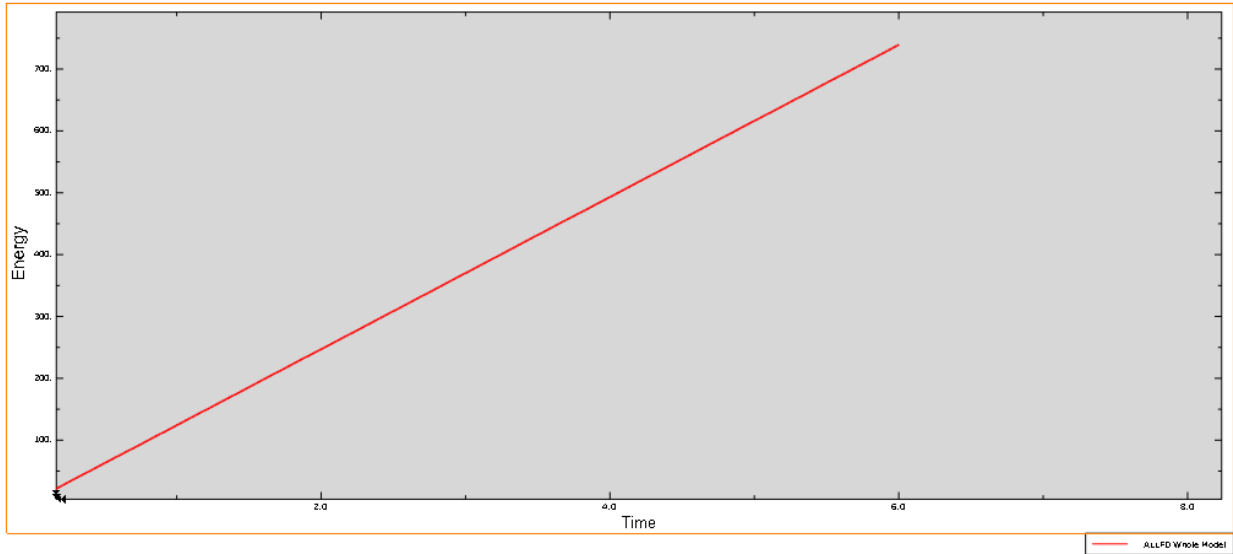


**Figure 4.8: Frictional dissipation energy**

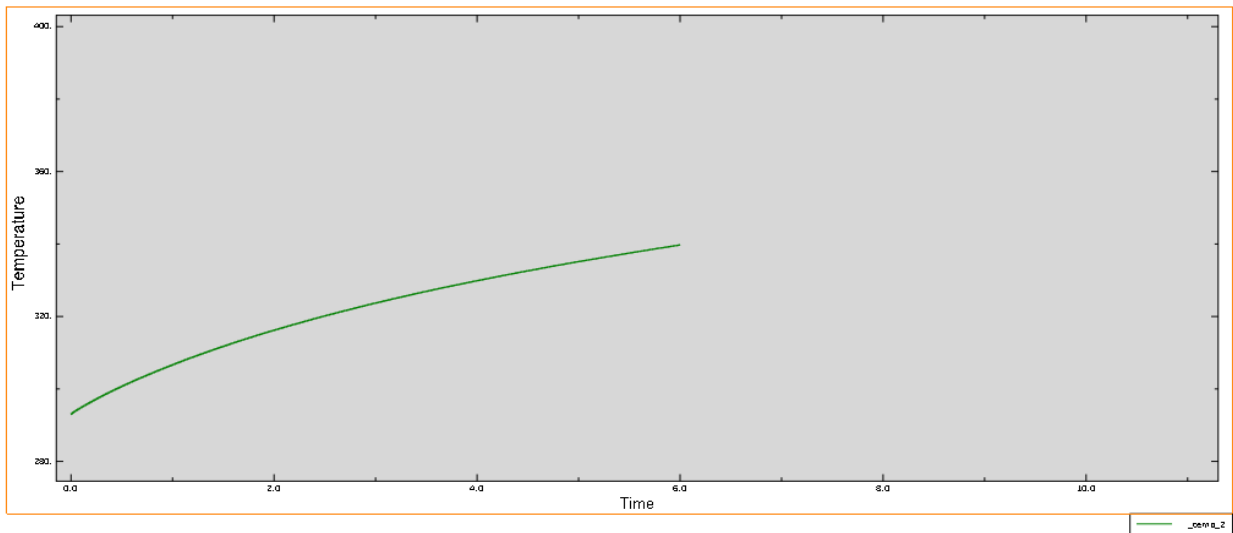


**Figure 4.9: Variation of temperature with time**

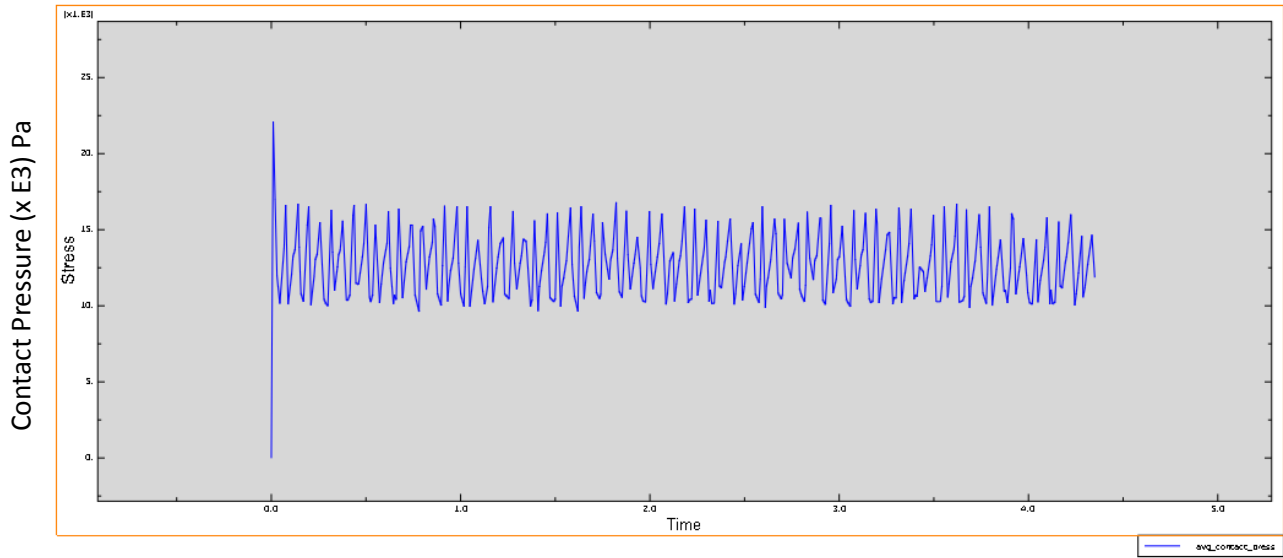


**Figure 4.10 Average contact pressure variations**

# CHAPTER 5

## RESULTS AND DISCUSSION

### 5.1 Wear rate

Wear mass has been converted into wear volume. Dividing wear volume by time, wear rate is obtained. The wear rate for different loads and different velocities are computed and plotted as show below.

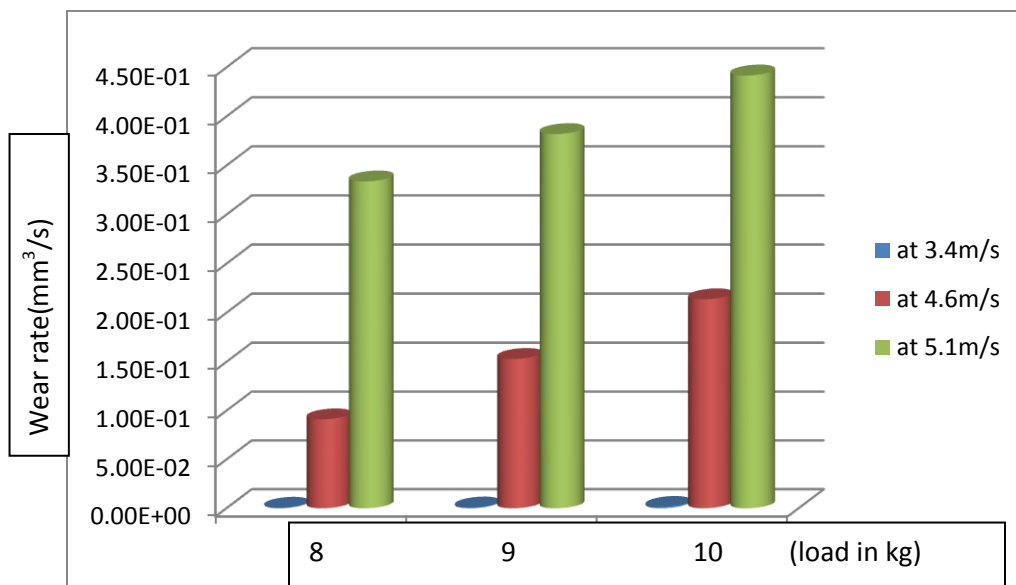


**Figure 5.1 Wear rate variation with load**

For the Figure 5.1, at a velocity of 3.4m/s wear rate is very small (in the power of E-3) which is shown in blue color. Wear rate at velocity of 4.6m/s and 5.1m/s are represented by red color and green color respectively. The wear rate is highest for velocity of 5.1m/s at 10kg load and lowest for velocity 3.4m/s at load of 8kg.

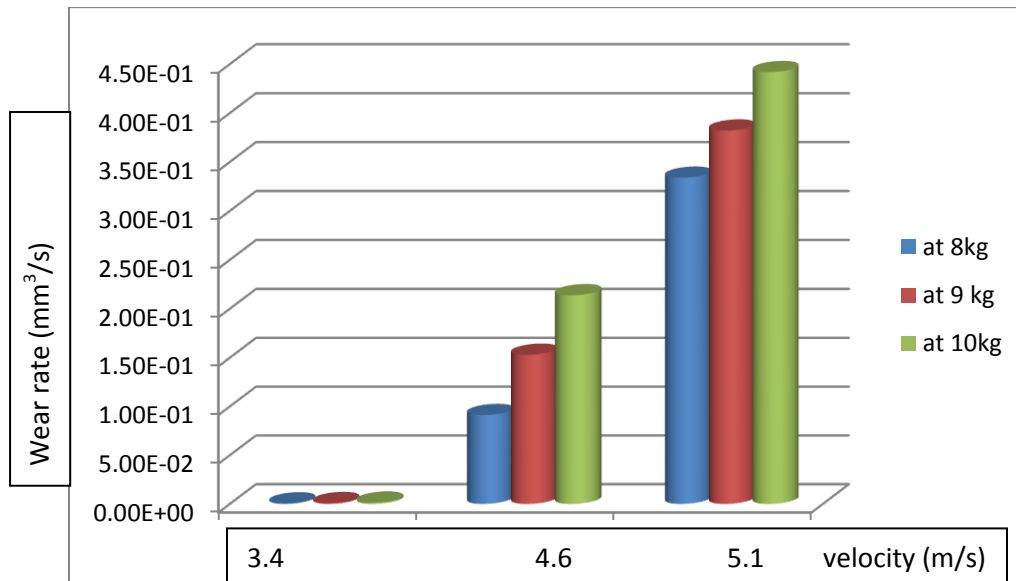


**Figure 5.2 Wear rate variation with velocity**

From the Figure 5.2, at velocity of 3.4m/s, as load increases wear rate also increases but this increase is very small. When the velocity is increased to 4.6m/s there is a significant change in wear rate with change in load.

## 5.2 Temperature

The bar graph shown below represents the comparison of variation of temperature at a velocity of 3.4m/s. Blue color represents the variation of temperature reading computed by Abaqus whereas the bar in red color represents the temperature measured by a thermographic imager.

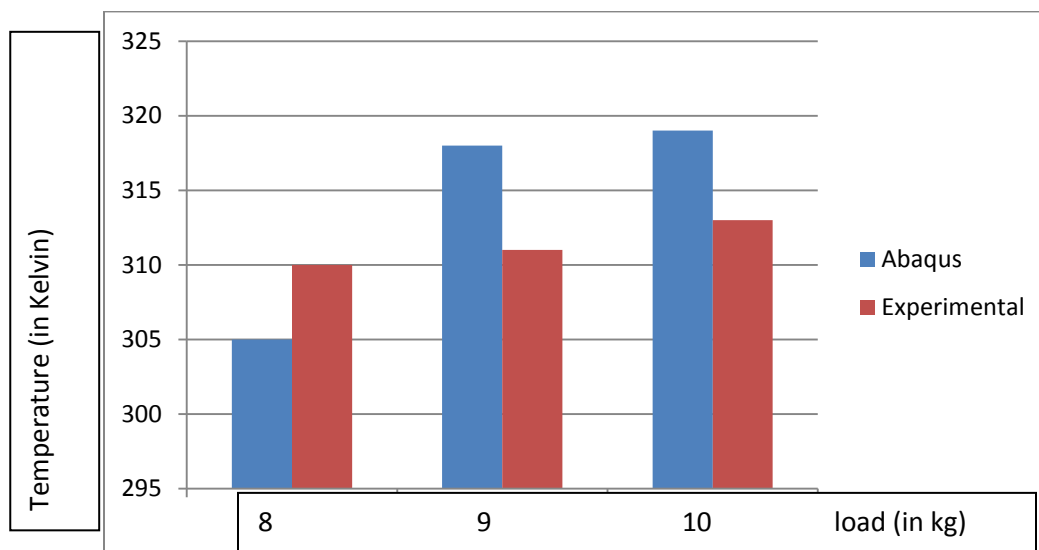


**Figure 5.3 Temperature at velocity of 3.4m/s**

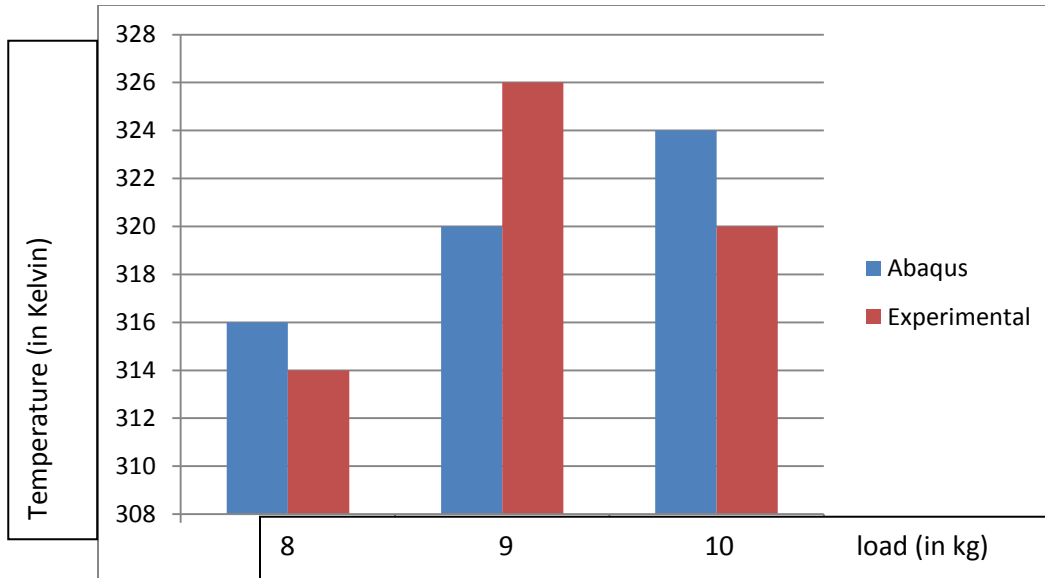


**Figure 5.4 Temperature at velocity of 4.6m/s**

The above bar graph represents the variation of temperature measured by thermographic imager and Abaqus at sliding velocity of 4.6m/s. There is slight deviation in the temperature. The reason is discussed in the next chapter.

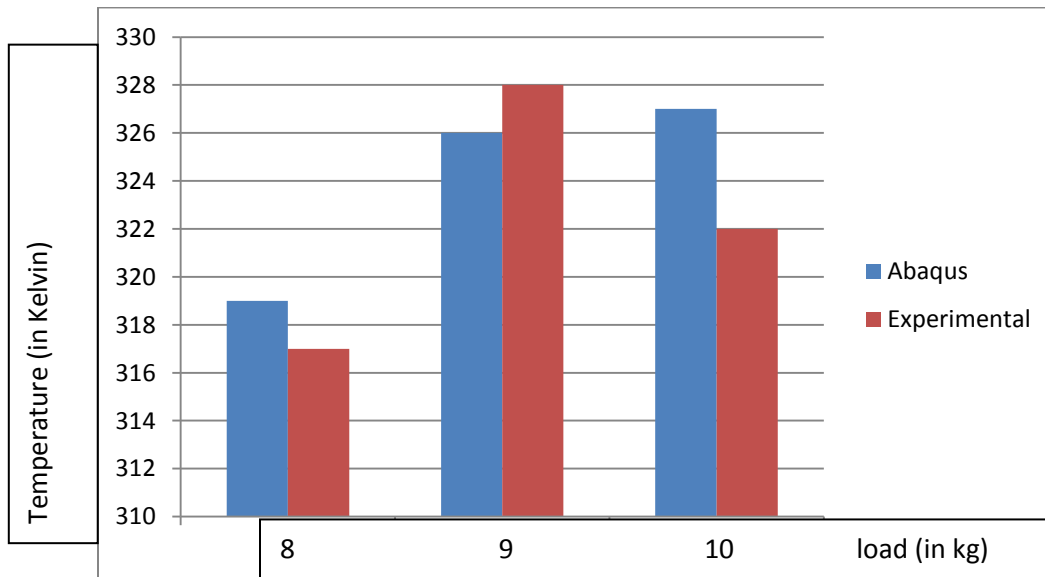


**Figure 5.5 Temperature at velocity of 5.1m/s**

Temperature measured by Thermographic imager and Abaqus are shown above for comparison at sliding velocity of 5.1m/s.



## CONCLUSION AND FUTURE PROSPECTIVE

The experiment was conducted for different loads at different sliding velocities and following conclusions can be drawn:-

1. From wear rate vs load bar graph, we can conclude that as load increases wear rate also increases i.e. wear rate is directly proportional to applied load.
2. From wear rate vs sliding velocity bar graph, it can be seen that as sliding velocity increases wear rate also increases.
3. There is frictional penalty between two contacting surfaces. So heat will be generated when pin slides over disc. This is passed to the pin as well as disc. Temperature rise of the disc is very small in comparison to pin because contact time is less but pin temperature first increases and then becomes nearly constant. This is due to the fact that heat generated due to friction will be lost in the atmosphere through convection and radiation.
4. Also there is some error in temperature measured by experiment and abaqus. There may be two reason for this:-
  - a) The coefficient of friction changes as sliding distance increases but it is assumed constant in abaqus.
  - b) The heat transfer coefficient used in abaqus may be different from the actual heat transfer coefficient

### Future Prospective

Tribology is the vast field of science, simulation of tribological problem gives a numerical analysis of the tribological problems and real life. The main future perspectives of this research work are as follows.

- a) Different combination of alloying elements can used to predict the wear behavior and temperature variations.
- b) Different coding method like FORTRAN or PYTHON scripts can be used to determine the wear rate and wear volume.
- c) The validity of experimental results can also be verified by other simulation software like ANSYS, NASTRAN, etc.

## REFERENCES

1. Theo Mang, Kirsten Bobzin and Thorsten Bartels(2010). “*Industrial Tribology: Tribosystems, Friction, Wear and Surface*” volume 1,pp.197-230.
2. “Wear.” Wikipedia.org. web. 19 Jul. 2017.<<https://en.wikipedia.org/wiki/Wear>>
3. “Review of plasticity” nptel.ac.in. 19 Jul. 2017, <<http://www.nptel.ac.in/courses/105108072/4>>
4. “Wear Mechanism”, nptel.ac.in, 20 Jul. 2017. <<http://nptel.ac.in/courses/112102015/11>>
5. Gwidon W. Stashowiak, Andrew W. Batchelor and Grazyna B. Stachowiak, text book of “*Experimental Methods in Tribology*”.
6. Bortoleto, E. M., Rovani, A. C., Seriacopi, V., Profito, F. J., Zachariadis, D. C., Machado, I. F., & Souza, R. M. D. (2013). *Experimental and numerical analysis of dry contact in the pin on disc test*. Wear, 301(1), 19-26.
7. Kennedy, F. E., Lu, Y., & Baker, I. (2015). *Contact temperatures and their influence on wear during pin-on-disk tribotesting*. Tribology International, 82, 534-542.
8. Li, X., Sosa, M., & Olofsson, U. (2015). *A pin-on-disc study of the tribology characteristics of sintered versus standard steel gear materials*. Wear, 340, 31-40.
9. Verma, P. C., Menapace, L., Bonfanti, A., Ciudin, R., Gialanella, S., & Straffelini, G. (2015). *Braking pad-disc system: Wear mechanisms and formation of wear fragments*. Wear, 322, 251-258.
10. Zmitrowicz, A. (2006). *Wear patterns and laws of wear—a review*. Journal of theoretical and applied mechanics, 44(2), 219-253.
11. S.Guicciardi, C. Melandri, F. Lucchini, G. De Portu, “*On data dispersion in pin-on-disk wear tests*”, Wear 252 (2002) 1001–1006.
12. Priit Poõdra, Soõren Andersson, “*Simulating sliding wear with finite element method*”, Tribology International 32 (1999) 71–81.
13. P.Prabhu et al, “*Experimental Study and Verification of Wear for Glass Reinforced Polymer using ANSYS*”.
14. ImamSyafa at al, “*Prediction of Sliding Wear of Artificial Rough Surfaces*”.
15. Lim, S. C., Ashby, M. F. and Brunton, J. H., *Wear-rate transitions and their relationship to wear mechanisms*. Acta Metall.,1987, 35, 1343–1348.

16. 'ASTM G 99 – 04: Standard Test Method for Wear Testing with a Pin-on-Disc Apparatus', ASTM International.
17. Singh, R. C., Pandey, R. K., Rooplal, Ranganath, M. S., & Maji, S. (2016). "Tribological performance analysis of textured steel surfaces under lubricating conditions". *Surface Topography: Metrology and Properties*, 4(3), 34005.
18. Mishra, P. C., Pandey, R. K., & Athre, K. (2007). "Temperature profile of an elliptic bore journal bearing". *Tribology International*, 40(3), 453–458.
19. Bijwe, J., Indumathi, J., John Rajesh, J., & Fahim, M. (2001). "Friction and wear behavior of polyetherimide composites in various wear modes". *Wear*, 249(8), 715–726.
20. Rajesh, J. J., Bijwe, J., Tewari, U. S., & Venkataraman, B. (2001). "Erosive wear behavior of various polyamides". *Wear*, 249(8), 702–714.
21. Rajesh, J. J., Bijwe, J., & Tewari, U. . (2002). "Abrasive wear performance of various polyamides". *Wear*, 252(9–10), 769–776.
22. Bijwe, J., Indumathi, J., & Ghosh, A. K. (2002). "On the abrasive wear behaviour of fabric-reinforced polyetherimide composites". *Wear*, 253(7–8), 768–777.
23. Kónya, L., Váradi, K., & Friedrich, K. (2005). "Finite element modeling of wear process of a peeksteel sliding pair at elevated temperature". *Periodica Polytechnica, Mechanical Engineering*, 49, 25 -38.
24. Podra, P. (1997). "FE Wear Simulation of Sliding Contacts". PhD thesis, Royal Institute of Technology (KTH), Stockholm, Sweden.
25. Yan, W., O'Dowd, N. P., & Busso, E. P. (2002). "Numerical study of sliding wear caused by a loaded pin on a rotating disc". *J. Mech. Phys. Sol.*, 50, 449-470.
26. Sumit Khot, Utpal Borah (2013), *International Journal of Science and Research (IJSR)*, "Finite Element Analysis of Pin-on-Disc Tribology Test"
27. Mathew Baby and Dr.K.R Jayadevan (2013), "Finite Element Modelling of Sliding Contact Wear in Aluminium", *Proceedings of International Conference on Materials for the Future - Innovative Materials, Processes, Products and Applications – ICMF 2013*
28. Hegadekatte, V., Huber, N., & Kraft, O. (2005). "Finite element based simulation of dry sliding wear. *Modeling Simul*". *Mater. Sci. Eng.*, 13, 57-75.

29. Bergan, P. G., Hørrigmo, G., Bråkeland, B., & Sørensen, T. H. (1978). "Solution techniques for non-linear finite element problems. *International Journal for Numerical Methods in Engineering*", 12(11), 1677-1696.
30. Benabdallah H. and Olender D., (2006). "Finite Element Simulation of the Wear of Polyoxymethylene in Pin-On-Disc Configuration", *Wear*, 261 pp. 1213-1224.
31. Singh RC, Pandey RK and Maji S (2013) "Experimental studies for accessing the influence of micro-dimple area density on tribological performance of mating contacts" *Int. J. Adv. Res. Innov.* 11-12.
32. Singh R C, Chaudhary R, Pandey R K and Maji S (2012). "Experimental studies for the role of piston rings' face profiles on performance of a diesel engine fueled with diesel and jatropha based biodiesel" *J. Sci. Ind. Res.* 71 57-62
33. Ranganath MS, Singh RC, Chaudhary R and Pandey RK(2014). "Experimental investigation of friction and wear behavior at the interface of aluminium and mild steel" *Int. J. Adv. Res. Innov* 2 775-80
34. Venkatesh, R., Rao, V. Seahagiri, Arunkumar, N., Biswas, S., & Kumar, R. S. (2015). "Wear Analysis on Silicon Carbide Coated HSS Pin on SS Disc Substrate" *Procedia Materials Science*, 10, 644-650..
35. Sharma S, Bijwe J, Panier S and Sharma M(2015). "Abrasive wear performance of SiC-UHMWPE nano-composites—influence of amount and size *Wear*" 332-333 863-71
36. Aranganathan N, Mahale V and Bijwe J (2016). "Effects of aramid fiber concentration on the friction and wear characteristics of non-asbestos organic friction composites using standardized braking tests *Wear*" 354-355 69-77
37. Ying, S., & Yupeng, Y. (2017). "Temperature field analysis of pin-on-disk sliding friction test." *International Journal of Heat and Mass Transfer*, 107, 339-346.
38. Abaqus Analysis User's Guide 6.12,(2012)